Accuracy Evaluation and Stability of the NBS Primary Frequency Standards

DAVID J. GLAZE, HELMUT HELLWIG, MEMBER, IEEE, DAVID W. ALLAN,
STEPHEN JARVIS, JR., AND ARTHUR E. WAINWRIGHT

Abstract—The National Bureau of Standards has two primary standards for frequency and the unit of time. They are both cesium devices and are designated NBS-4 and NBS-5. The design of NBS-5 is discussed in detail, including its relationship to its predecessor NBS-III, and a brief description of NBS-4 is given. NBS-4 and NBS-5 have been used since January 1973 for a total of twelve calibrations of the NBS Atomic Time Scale.

The application of pulsed microwave excitation, and the use in the accuracy evaluations of frequency shifts due to known changes in the exciting microwave power are discussed. Measurements of the atomic velocity distributions are reported.

A stability of 9×10^{-15} derived from the comparison of NBS-4 and NBS-5 is reported for averaging times of 20 000 s, and data on accuracy are given. Results obtained to date give an evaluated accuracy of $1-2 \times 10^{-13}$ with indications that this accuracy may be improved in the future.

The bias-corrected frequencies of NBS-4 and NBS-5 agree to within $(1 \pm 10) \times 10^{-13}$ with the value obtained for NBS-III in 1969—which value is preserved in the rate of the NBS Atomic Time Scale.

INTRODUCTION

A primary cesium-beam frequency standard serves to realize the unit of time, the second, in accordance with the international definition as formulated at the XIII General Conference of Weights and Measures in 1967: "The second is the duration of 9 192 631 770 periods of the radiation corresponding to the transition between the two hyperfine levels of the ground state of the cesium-133 atom." The realization of an output frequency from a real device involves several steps of physical and technical processing which may cause a frequency deviation of the output frequency from the unperturbed atomic transition frequency. The magnitude of each such bias can be evaluated with the aid of experiments and theoretical considerations. However, these biases are not known exactly. The magnitude of these uncertainties depends on the degree of theoretical understanding as well as on the precision with which experimental parameters can be measured. This precision depends on two things. One is the design and construction of the cesium-beam tube and electronics of the primary frequency standard; the other is the frequency stability of the reference standard used in the evaluation of the primary standard. The combined uncertainty of all biases is referred to as the accuracy of the frequency standard.

The experience gained with NBS-III indicated that the main internal limitations for accuracy, in addition to significant electronics problems, were the magnetic field, in particular its homogeneity and stability, the second-order Doppler effect, and the cavity phase-angle difference (large for NBS III) [1]. The principal external limitation to accuracy was lack of a suitable high performance standard against which to measure for evaluation of the various parameters of the primary standard. It was possible, for example to evaluate NBS-III to 5×10^{-13} [1], using various types of commercial standards at NBS. The development of both NBS-4 and NBS-5 was initiated in late 1965 and early 1966,[1] with the intent to improve significantly both the accuracy and stability.

NBS-5 was designed with an accuracy goal of 1 part in 10^{13}. To facilitate accuracy evaluations, designs of both NBS-4 and NBS-5 also aimed at improving the frequency stability by at least one order of magnitude. This stability is basically governed by the available atomic beam intensity and the resonance line Q. The stability for 1 s sampling time of NBS-III was 1.2 parts in 10^{11}. The stability of either NBS-4 or NBS-5 is limited by shot noise of the detected cesium beam itself. The NBS-4 fractional frequency stability can be characterized by $\sigma_y = 1.5 \times 10^{-12} \tau^{-1/2}$ and the NBS-5 stability by $\sigma_y = 8.5 \times 10^{-13} \tau^{-1/2}$, where σ_y is the square root of the Allan Variance and τ is the sample time ($1 \text{ s} < \tau < 10^4 \text{ s}$). The σ_y values are for each primary standard by itself, and were derived from actual intercomparisons of NBS-4, NBS-5 and new, low-noise commercial quartz-crystal oscillators.

THE NBS-5 BEAM TUBE

A photographic view of NBS-5 with all electronics is depicted in Fig. 1. For comparison, a photograph of NBS-III is shown in Fig. 2. The complete NBS-5 system

[1] NBS-4 was constructed in a joint effort by NBS and the Hewlett–Packard Company. A contract was awarded to Hewlett–Packard to aid in the development. This cooperative effort involved construction and assembly by personnel from both Hewlett–Packard and NBS. This device, however, was not originally intended to be used as a primary cesium-beam frequency standard. New techniques, however, coupled with its design quality and high stability, permit its use as a primary standard [2]. NBS-4 and NBS-5 will continue to be used as primary frequency standards for measurements involving the NBS Atomic Time Scale. NBS-III was totally dismantled in 1970, and parts of its vacuum system are used in NBS-5.
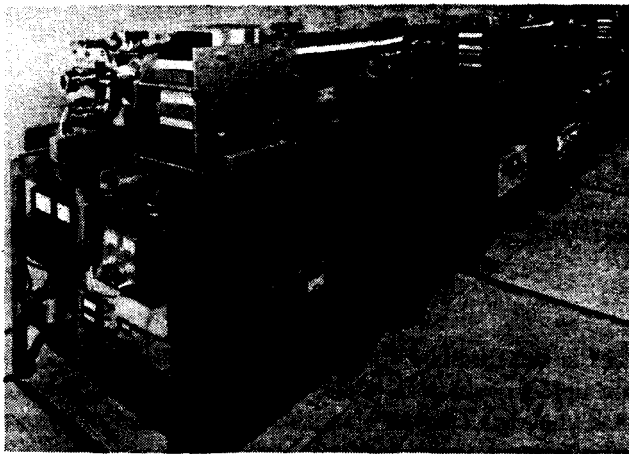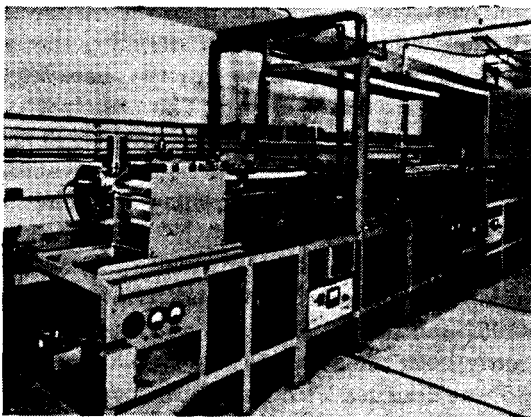
Fig. 1. NBS-5. All electronic systems are shown.

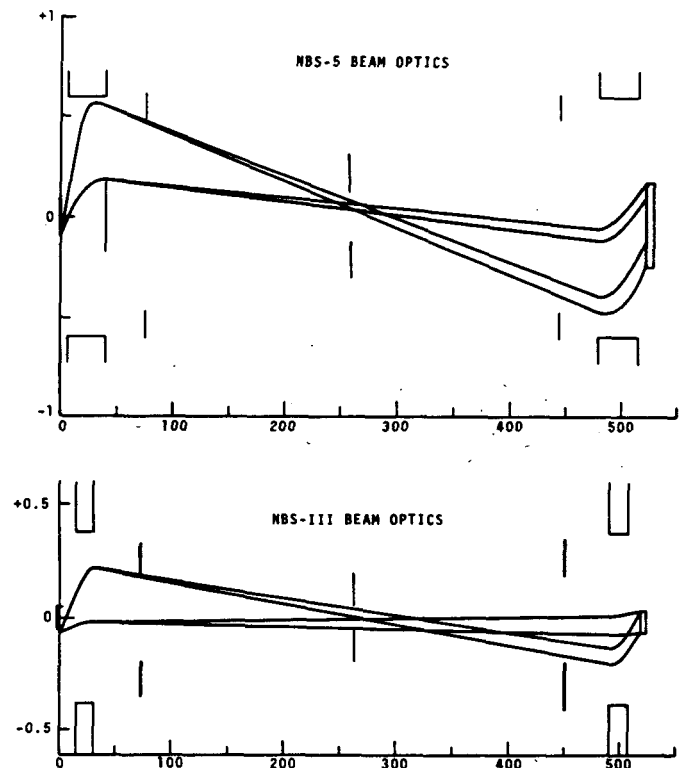Fig. 2. NBS-III. Frequency-lock electronic systems are not shown.

Fig. 3. Beam optics comparisons of NBS-5 and NBS-III. Scales are in centimeters. Cavity and center slit apertures together with NBS-5 beam stop are designated by vertical lines. Magnet gaps are represented by unclosed rectangles, while detectors are shown by closed rectangles. Collimator for NBS-5 is series of dots, while uncollimated source for NBS-III is unclosed rectangle.

has a length of about 6 m overall. The vacuum system is basically a stainless steel tube, 25 cm in diameter, and is evacuated by three 200 1/s ion pumps which can be closed off with valves for servicing of the pumps.

Fig. 3 gives a schematic view and a comparison of the beam alignments in NBS-5 and NBS-III. In contrast to the NBS-III design, a beam stop at the exit of the first NBS-5 magnet is used to reduce background due to fast atoms reaching the detector along the line of sight. This location for the beam stop gives both maximum filtering of fast atoms with minimal effect on slower atoms and minimum cesium deposition on the inner walls of the cavity. Such deposition can lead to a variable phase angle difference between the interaction regions and to attendant frequency fluctuations [1]. Also indicated in Fig. 3 are the two limiting trajectories of the highest and lowest velocities of atoms (originating from a particular collimator opening) which successfully reach the detector. In the drawing, it is assumed that transitions are induced in the cavity region which cause a change of state in all the atoms. The figure gives the trajectories of useful[2] atoms leaving the oven in only one of the two atomic

states which participate in the transition. The other state is also utilized (but not shown) and has corresponding trajectories, starting below the optical axis of Fig. 3, and then crossing over at the center aperture of the tube. The center aperture thus is reasonably well located at the crossover of the trajectories of all velocities for the two states.

The cavity and magnetic shield structures are shown schematically in Fig. 4. The basic C-field design is similar to that of NBS-4 (although NBS-4 has no Armco shield), and is attributable to and patented by Lacey et al. [3]. The cavity and magnetic shields are located inside of the vacuum system in order to assure mechanical stability and to reduce thermal effects. The length of the Ramsey-type cavity is 3.74 m. One of the most critical parameters of the beam tube is the phase angle difference between the two interaction regions of the cavity. For the first time at NBS, this parameter was carefully trimmed before assembly of the tube. The trimming was done by separate measurements of the cavity components: interaction regions, arms, and E-plane tee. The testing and further corrective actions continued during the assembly of these cavity components. The electrically measured cavity phase angle difference was less than 1 mrad at the time of final assembly. This phase difference has not been adjusted since the assembly of NBS-5.

The magnetic-shield package consists of three separate magnetic shields: two of a box-like structure containing

---

[2] Useful atoms are those which both undergo the $(F = 4, m_F = 0) \leftrightarrow (F = 3, m_F = 0)$ transition and also reach the detector.
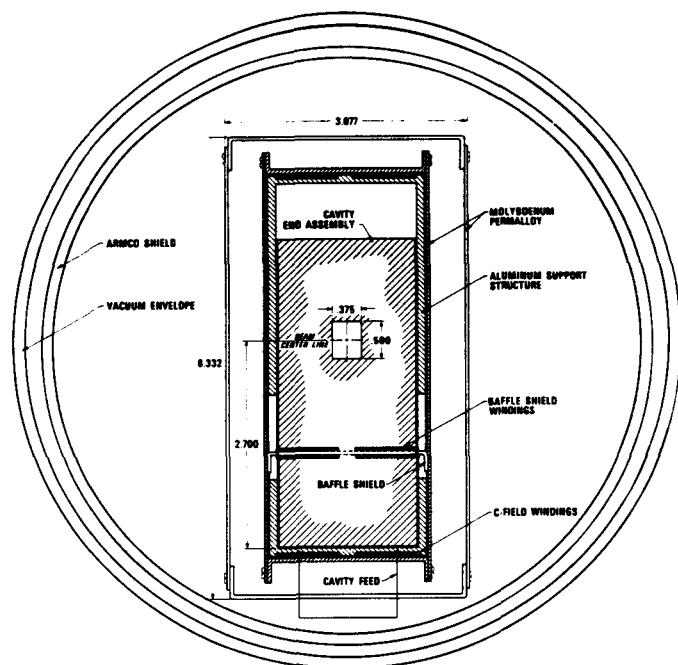
Fig. 4. Cross section scale drawing of NBS-5 beam tube. Dimensions are in inches. Cavity structure, aluminum support structure, and magnetic shields are all electrically insulated from one another except at the cavity feed. There they are all joined electrically to one point which is system ground. Baffle shield (and its windings) serve to shield beam from opening through which the cavity feed passes. Baffle shield and its windings are approximately 76 cm in length. Innermost rectangular molybdenum-permalloy shield and windings define the C-field region of 427 cm in length.
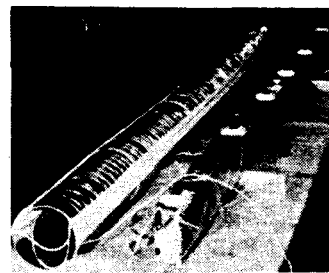

Fig. 5. View of NBS-5 microwave cavity/magnetic shield package before final assembly. Cylinder on left is outer shield; the box-like structure on right comprises the two inner shields and contains microwave cavity. (See Fig. 4.)
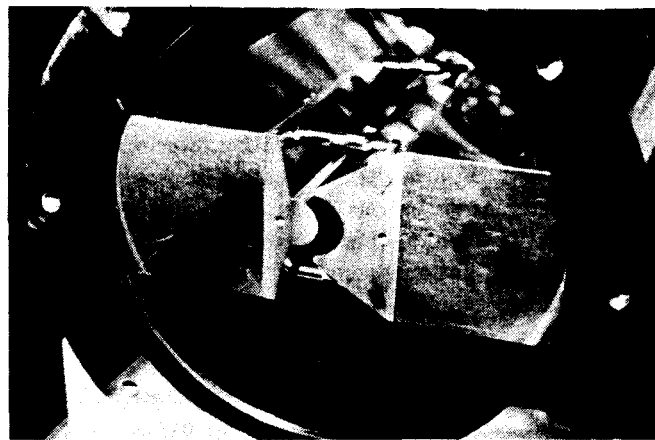

Fig. 6. View of one of NBS-5 dipole magnets. Gap-width 1.2 cm. Pole tips and return ring are soft iron; magnetic drivers, between pole tips and return ring, are Alnico-5.
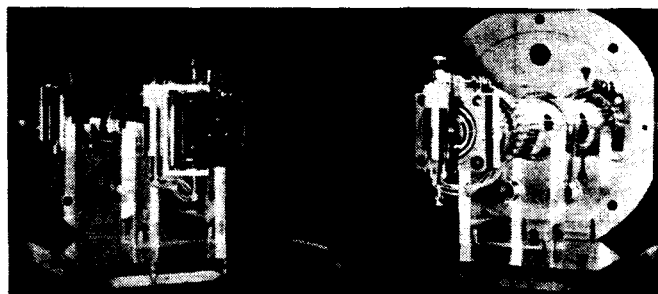

Fig. 7. View of oven/detector systems from both ends of NBS-5 beam tube, before final assembly. System on left is adjusted for "oven-mode," one on right for "detector-mode."

the microwave cavity; the third outer shield of a cylindrical design. The shields, microwave cavity, and vacuum system are all electrically insulated from one another except at the center of the beam tube where all are joined at one point which is the system ground. Fig. 5 depicts the structures before final assembly. The typical operating field is about 4.8 A/m (60 mOe), and a field homogeneity of better than 1-percent peak-to-peak along the tube axis was measured with a field probe after assembly.

The deflection magnets are shown in Fig. 6. They have a length of 35 cm and a gap of 1.2 cm (measured at the center). The pole-tip configuration reproduces a two-wire field, and the peak field strength at the pole tip is about 0.93 T (9.3 kG). Trimmers are located on the cavity side of the magnets and are carefully adjusted to assure a smooth transition (in strength as well as orientation) from the high magnetic field of the magnet through the magnetic-shield end caps into the shielded cavity region, thus avoiding Majorana effects. The beam tube permits an atomic beam to traverse the path through the cavity in either direction. Each end of the beam tube is equipped with identical magnets and oven-detector combinations. For beam reversal the beam stop, shown in Fig. 3, can be withdrawn and a second beam stop can be inserted at the other magnet. This capability of beam reversal was introduced in order to provide the system with the capability of an additional measurement of the cavity phase-difference bias: the frequency bias changes sign if the beam

traverses the cavity in the opposite direction. The oven-detector combination, depicted in Fig. 7, is arranged in such a way that it can be adjusted in the deflection plane of the atomic beam, perpendicular to the beam axis; in addition, the oven can be aimed independently at different angles. The oven can accept ampules filled with up to 8 g of cesium. The collimator of the oven is an array of about 500 separate channels producing a beam with a rectangular cross section of 2 mm × 9 mm. With an oven temperature of 100°C, the projected beam intensity at the detector is approximately 10^8 atoms per second. The ionizer is composed of 90-percent Pt and 10-percent Ir and is a ribbon 0.025 mm in thickness and 4.06 mm in width. This ribbon operates at a temperature of 950°C.

The ionizer ribbons can be heated to this temperature in air and then later used successfully without failure in the beam tube. Indeed no ionizer failures have occurred in NBS-5 during its one and one-half year life of nearly continuous operation. This improved ionizer performance has been a major factor in reduction of down-time compared with the NBS-III system. Because of the relatively high beam intensity (15 pA) and the high purity of the platinum ribbon (total background current is of the order of 0.1 pA), no mass spectrometer and electron multiplier are employed. Instead, a field-effect transistor is mounted in close proximity to the detector. The detector signal is processed in low-noise preamplifiers external to the beam tube. As designed, if one end operates in the "oven" mode the detector is moved aside; however, if that end is used in its "detector" mode, the detector can move in front of the oven. At the same time, a carbon getter plate baffles the oven collimator (see Fig. 7). Lowering the oven temperature to approximately room temperature at this end also reduces its output. There have been some problems with the beam reversal system as designed due to cesium contamination; consequently, modifications are being made to improve performance in this area.

THE NBS-4 BEAM TUBE

A view of NBS-4 with electronics systems is shown in Fig. 8. The NBS-4 beam tube has an overall length of about 1.5 m, with a Ramsey cavity interaction length of 52.4 cm. The vacuum system is a stainless steel tube, about 25 cm in diameter, and is evacuated by a single 140 l/s ion pump. Operating pressure is typically 2.7×10^{-7} N/m^2 (2×10^{-9} torr).

Fig. 9 gives a general schematic view of the beam optics design of NBS-4. This design utilizes an offset geometry, and as a result, beam stops and a center slit (as used in NBS-5) are not necessary for filtering very high velocity atoms. In general, atoms reaching the detector may make a transition only in one direction between the ($F = 4$, $m_F = 0$) and ($F = 3$, $m_F = 0$), hyperfine levels.

The cavity and magnetic shield structures for NBS-4 are similar to those shown in Fig. 4, although dimensions are different. Neither an aluminum support structure nor an Armco shield is used. As in NBS-5 the phase angle difference between the two interaction regions of the cavity was carefully trimmed to be less than 1 mrad before assembly of the beam tube.

The deflection magnets are of a dipole design, with a length of 8.9 cm and a gap of about 0.6 cm. The peak field strength at the convex pole tips is about 1.5 T (15 kG). Trimmers are located on the cavity side of each magnet, and are carefully adjusted to assure a smooth transition (in field strength as well as field orientation) from the high magnetic field of the magnet through the magnetic shield end caps into the shielded cavity region, thus avoiding Majorana effects. Uncertainties due to the C-field related biases cause a total contribution to inaccuracy of less than 5×10^{-14}. This is also true for NBS-5. The microwave spectrum is re-checked infrequently, since
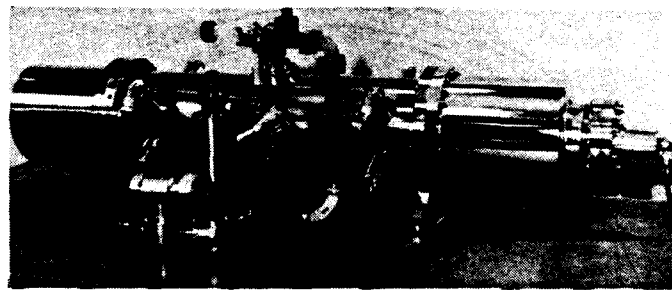

Fig. 8. NBS-4 beam tube. Cesium oven is inside left end bell, while cesium beam detector is inside right end bell. Low-noise field-effect transistor (operating as source follower) is mounted in connector (on the right end) just outside of vacuum flanges. All electronics systems and vacuum pump are supported by frame below the beam tube.
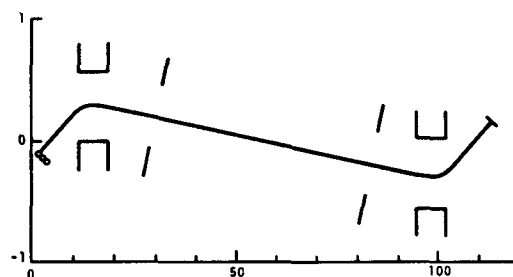

Fig. 9. Schematic drawing of NBS-4 beam tube geometry. Scales are in centimeters. Magnet pole tip locations are represented by unclosed rectangles. Cavity apertures and ionizer ribbon are indicated by straight lines. Collimator openings are represented by row of circles (not to scale). Solid line from collimator to ionizer is intended only to show possible trajectory taken by useful[2] atom.

the C-field parameters are very stable over long periods of time. Indeed over a month's time the frequency offset of the ($F = 4$, $m_F = \pm 1$) $\leftrightarrow$ ($F = 3$, $m_F = \pm 1$) field sensitive transitions which are used to calibrate the C-field bias, changes only about 2 Hz. This amounts to an error in the frequency of the ($F = 4$, $m_F = 0$) $\leftrightarrow$ ($F = 3$, $m_F = 0$) transistion of only 1.6×10^{-14}. Even though these changes are small, and are due in large part to the C-field current source, they are properly accounted for in all frequency calibrations.

It is possible to reverse the beam in NBS-4; however, this can only be done by opening the vacuum chamber and demounting the oven/A magnet assembly and interchanging it with the detector/B magnet assembly. Some rewiring is necessary as well. Since this is a fairly long procedure, and since beam reversal data have been obtained and evaluated from NBS-5 (in the light of the pulse method and power-shift method [2]), the beam has not been reversed in NBS-4. However, independent accuracy data on NBS-4 were obtained solely by the power-shift method. Also, beam reversals which permit the vacuum system to be opened to the atmospheric environment can lead to errors in the determination of the cavity phase shift bias [1]. NBS-4 has some unique features which will permit evaluation of cavity phase-shifts possibly occurring over the beam cross-section [4], [5]. These

experiments will be pursued in the near future, since the more conventional evaluation phase is completed for NBS-4.

The ionizer and collimator in NBS-4 are very similar to those in NBS-5; however, the cesium oven charge in NBS-4 is about 1 g. This will provide over one year of continuous operation at signal intensities of about 10^8 atoms per second at the detector (at an oven temperature of about 100°C). To date, NBS-4 has been operated for about seven months on its first oven charge.

A more complete discussion of the detailed design of NBS-4 is planned in a future publication.

ELECTRONICS SYSTEMS AND FREQUENCY STABILITY

The microwave signals for both NBS-4 and NBS-5 are obtained from crystal oscillators at a basic frequency of 5 006 880 Hz, a subharmonic of the cesium transition frequency. In the electronic system of Fig. 10, which is applicable to either standard, the oscillator drives an associated low-noise multiplier chain which in turn drives a step recovery diode producing a signal at the cesium resonance frequency with a power of up to 10 mW. However, only about 50 μW of power is necessary to drive the atomic transitions optimally; therefore, about 20 dB of attenuation is used between the chain output and the microwave cavity. The older klystron and primary-loop phase-lock systems [1] have now been eliminated and all systems are now redesigned with solid-state components. Phase-noise measurements for these new multiplier systems are shown in Fig. 11. A sinusoidal frequency modulation can be applied with a fundamental frequency of 18.75 Hz. This modulation is generated with second-harmonic suppression (measured) of better than 100 dB with respect to the fundamental modulation level. The modulation reappears in the beam current at the detector, is amplified, phase detected, and processed in two cascaded integrators and used to servo-control the crystal oscillator. (The original idea and design for the double integrator was first proposed by Cutler [6]). The double integrator technique provides such a high loop gain at very low frequencies—essentially dc—that offsets due to finite correction voltage on the oscillator varicap are reduced to less than 1×10^{-14} in their effects on the output frequency for any reasonable, continuous operational period (months to years). The only difference in the two electronic systems are slight differences in servo loop gain and integrator time constants which are tailored to each particular beam tube, taking into account resonance linewidths and signal-to-noise ratios. The 5 006 880-Hz crystal oscillator frequency is also separately synthesized to a standard 5 000 000-Hz frequency. This signal is used for evaluative and stability measurements, and for time scale calibrations.

During 1973, measurements taken on both the NBS-4 and NBS-5 complete systems indicated that neither system permitted as good short-term stability as measurements of the figures of merit of the beam tubes alone
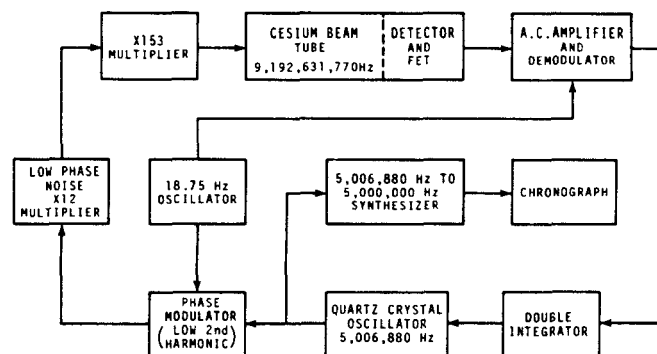

Fig. 10. Block diagram of electronics systems used for both NBS-4 and NBS-5. All components are solid state, and throughout systems, low-noise design concepts were followed. For example, phase noise measurements for the frequency multiplier are described in Fig. 11, and in [1].
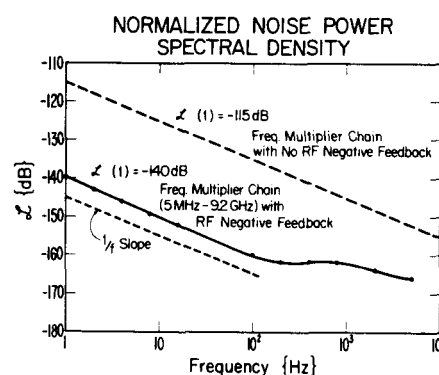

Fig. 11. Measurements showing phase-noise level for individual frequency multiplier chains used in both NBS-4 and NBS-5 systems. Multiplier chains use local, RF negative feedback to reduce phase noise level to -140 dB at 1-Hz Fourier frequency, in 1-Hz measurement bandwidth. Measurements are described, and $\mathcal{L}$ is defined in [1].

predicted. (See [7] for definitions of figure of merit). The figure of merit of 60 measured for NBS-4 would lead one to expect a $\sigma_{y\text{NBS-4}}$ at $\tau = 1$ s of 1.4 parts in 10^{12}. From the figure of merit of 150 measured for NBS-5 one would expect $\sigma_{y\text{NBS-5}}$ to be 5.6 parts in 10^{13} at $\tau = 1$ s.[3] Fig. 12 shows the large discrepancies between measured and predicted performance. The source of the problem was in the 5 006 880-Hz quartz-crystal oscillators of both systems—phase-noise levels generated in the oscillator electronics were masking the shot-noise levels of the cesium detection process.

In early 1974, the 5 006 880-Hz commercial oscillators described were replaced with new commercial quartz-crystal oscillators operating at the same frequency but displaying a 20-dB improvement in the phase-noise levels.

The short-term stabilities then obtained for the individual NBS-4 and NBS-5 systems are shown in Fig. 13,

---

[3] A figure of merit of 200 has been measured for NBS-5, early in 1973. However, due to vacuum pumping limitations and cesium getter problems, some beam scattering is evidently occurring which has reduced the figure of merit to a stable 150. Modifications are underway to reduce beam scattering and to improve the performance of the beam reversal system.
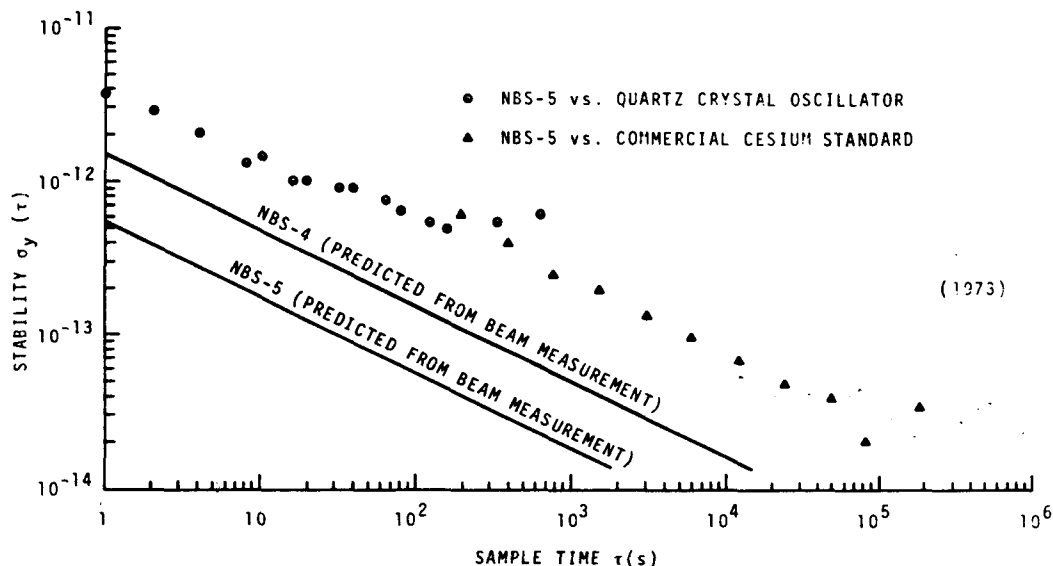
Fig. 12. Short-term frequency stability data of NBS-5 during period when phase noise of locked quartz-crystal oscillator (Fig. 10) was predominant. These oscillators have been replaced by other commercial units with lower phase-noise levels which permit system noise to approach fundamental shot-noise (solid lines) of cesium beam itself. (See Fig. 13.)
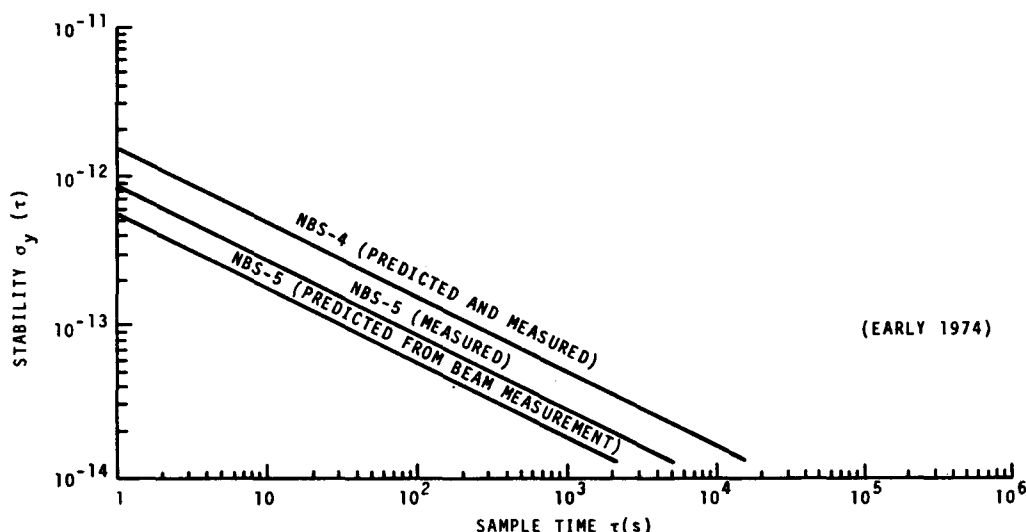

Fig. 13. Short-term frequency stability (both measured and predicted) for individual NBS-4 and NBS-5 systems. Individual data points are not shown, to preserve clarity. Line drawn for "NBS-5 predicted from beam measurement" is based on measured figure of merit of 150 (see [7]) for NBS-5.

and again compared with prediction. These data were again obtained in round-robin measurements using the unlocked low-noise quartz-crystal oscillator in the NBS-5 system as a reference for the locked NBS-4 system and vice-versa. Short-term stability data were also obtained by comparison of the free-running quartz-crystal oscillators over the same time intervals ($1 \text{ s} < \tau < 100 \text{ s}$). Tests were made to insure that the noise levels from these two oscillators were at comparable levels. It was then possible from these data to deduce the short-term stability for NBS-4 and NBS-5 individually. Additionally, direct comparisons between NBS-4 and NBS-5 were made and these data are characterized by $\sigma_y(\tau) = 1.7 \times 10^{-12}\tau^{-1/2}$.

This is the level expected if one combines statistically the individual curves for NBS-4 and NBS-5 shown in Fig. 13. It is clear that the full shot-noise limited capability for NBS-4 has been achieved, while the full potential of the NBS-5 beam tube has not quite been achieved. This is due to two factors: first, the noise of the new 5 006 880 Hz locked oscillator contributes a small amount to the noise level of the measurement, and second, the modulation rate of 18.75 Hz is somewhat too high to permit the full shot-noise limited performance to be realized. The development of new servo systems is planned which will permit these limitations to be overcome. Digital, square-wave frequency modulation techniques are being considered,
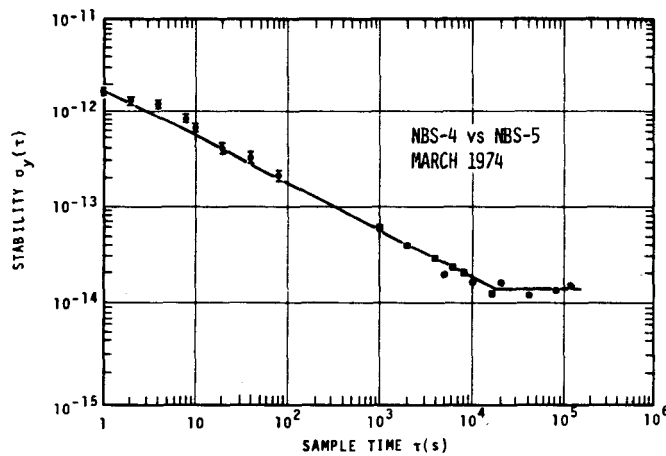
Fig. 14. Frequency stability data from comparisons of NBS-4 and NBS-5.

and some investigative work in this area has already begun at NBS.

In order to gain some information about long-term stability, NBS-4 and NBS-5 were compared during a few experiments for sample times between 100 s and 2×10^5 s. These data, together with some short-term data from the NBS-4/NBS-5 measurements described here, are shown in Fig. 14. The long- and short-term data points fit reasonably well to the line $\sigma_y = 1.7 \times 10^{-12} \tau^{-1/2}$. Also at sample times greater than 10^4 s, a "flicker floor" of $\sigma_y = 1.3 \times 10^{-14}$ is reached beyond which more averaging does not improve stability. In this region one cannot say which standard is the limitation; however, one can assume that one of them has a stability at least as good as $(1.3 \times 10^{-14})/\sqrt{2}$. If this is done, then the best stability achieved for one is about 9×10^{-15} for 10^4 s $< \tau < 10^5$ s. In the authors' opinions, the most probable reasons for the flicker floor in Fig. 14 are not fundamental limitations in the beam-tube itself, but rather effects due to environment and/or electronics systems. Experiments are planned toward a better understanding and reduction of the flicker level.

ACCURACY EVALUATIONS FOR NBS-4 AND NBS-5: JANUARY 1973–JUNE 1974

Contributions to accuracy are summarized in Table I. Because more information has been obtained and since better experiments are being done as time goes on, many of the bias uncertainties have been reduced compared to previous publications [9]. All biases (1σ) in Table I are nominally zero except for Items 1 and 3. For NBS-4 the bias in Item 1 is almost totally due to the second-order Doppler effect and amounts to -1.2×10^{-13}. The cavity phase angle difference is zero within a measurement uncertainty of 0.06 mrad. For NBS-5, in the present beam direction, the second-order Doppler and phase-shift biases are of opposite signs, and the net result is a bias of -1.6×10^{-13}. For Item 3, both NBS-4 and NBS-5 are operated with C-field magnitudes (60 mOe) which give a bias of

Accuracy Evaluation for NBS-4 and NBS-5: January 1973 - June 1974		
Influencing Factors	NBS-4 Uncertainty x_i	NBS-5 Uncertainty x_i
1. 2nd-order Doppler and phase difference at nominal optimum power; source: power shift, and pulse method.	2.8×10^{-13}	1.5×10^{-13} [4]
2. Servo system; source: variation of servo parameters and calculations based on measured offsets and loop gain.	1×10^{-13}	1×10^{-13}
3. Magnetic field; source: $m_F \neq 0$ transitions.	0.08×10^{-13}	0.08×10^{-13}
4. $(\overline{H})^2$ vs $\overline{(H^2)}$; source: $m_F \neq 0$ transitions degaussing tests, measurements during assembly, field trimming experiments, (no correction is applied - the bias is the uncertainty).	0.4×10^{-13}	0.4×10^{-13}
5. Majorana Transitions; source: $m_F \neq 0$ transitions and measurements during assembly.	0.05×10^{-13}	0.05×10^{-13}
6. Pulling due to neighboring lines; source: $m_F \neq 0$ transitions.	0.1×10^{-13}	0.05×10^{-13}
7. Cavity pulling; source: worst estimate.	0.5×10^{-13}	0.03×10^{-13}
8. Rf Spectrum; source: rf spectrum recording.	0.8×10^{-13}	0.04×10^{-13}
9. Random Uncertainty; source: Fig. 14.	0.1×10^{-13}	0.1×10^{-13}
Square root of sum of squares of uncertainties, x_i :	3.1×10^{-13}	1.8×10^{-13}

[4] Combination of Beam reversal and power shift measurements for one evaluative experiment.

$+1670.00 \times 10^{-13}$. This bias is routinely set to this value and monitored for each calibration—the bias uncertainty represents the stability with respect to the nominal bias value, over the course of an experiment, not one's ability to set to the bias value which is much better.

Item 2 in Table I is probably pessimistic; however, until an extensive group of experiments can be concluded using NBS-4 and NBS-5 as reciprocal references, the uncertainty for servo system effects is conservatively quoted as 1×10^{-13}.

The bias uncertainty for Item 4 in Table I has been estimated from data obtained both on C-field homogeneity at the time of assembly of NBS-4 and NBS-5 and on data from the microwave spectra ($m_F \neq 0$ transitions) of NBS-4 and NBS-5. The estimates are again pessimistic, and will be updated as investigations progress. It should be noted that for both NBS-4 and NBS-5 the C-field values at the interaction regions can be adjusted to agree as closely as desired to the field value in the drift region. Hence, no contribution for this effect appears in Table I, since one is limited only by his ability to set the fields—this certainly corresponds to a frequency bias $\leq 10^{-15}$ for the $(F = 4, m_F = 0) \leftrightarrow (F = 3, m_F = 0)$ transition.

Items 5 and 6 were estimated from appropriate data taken from the microwave spectra and direct field measurements on NBS-4 and NBS-5. Suitable expressions for calculation of these effects are given in [10].

Item 7 assumes for both NBS-4 and NBS-5, a cavity detuning of 0.1 MHz, which has been proven a pessimistic estimate even over long periods of time.

Item 8 arises from many measurements of the rf spectra of the excitation systems, and is based on $\frac{1}{2}$-dB asymmetry

in 60-Hz sidebands down at least 50 dB from the X-band carrier level, a conservative estimate.

The most notable contribution in Table I is the uncertainty in the velocity dependent biases: the second-order Doppler and cavity phase-shift biases. They are lumped together since their determination usually results from the same measurement procedure. Being the most significant limitation in the present accuracy budgets of both NBS-4 and NBS-5, their determination will be discussed in more detail in the following.

The total velocity dependent frequency bias is given by [2], [11]

$$\Delta\nu = -\tfrac{1}{2}\nu_0 \frac{V_D{}^2}{c^2} - \frac{\delta}{2\pi L} V_p \qquad (1)$$

where ν_0 is the atomic resonance frequency, c is the speed of light, δ is the cavity phase angle difference, and L is the distance between the centers of the two sections of the Ramsey cavity. The first term in (1) is the second-order Doppler term containing a mean-squared velocity $V_D{}^2$. The second term arising from the cavity phase shift is proportional to V_p, a mean of the linear velocities. Both V_D and V_p are not simple means of the velocity distribution alone, but also are dependent on the microwave power and the mode of servo-control [11]. Equation (1) can be used to determine the cavity phase angle difference if a frequency-shift measurement for at least two different, though known, settings of these velocities can be performed. In the following, we discuss the three methods which were used on NBS-4 and NBS-5 to effect such a controlled change in velocities.

1) Pulsed Operation: This evaluation technique was used once on NBS-5. The microwave power is applied in pulses of suitable length, power, and pulse frequency such that a narrow atomic-velocity range is selected in the beam tube [2], [8]. The tube is operated in the frequency standard mode (i.e., locked), and the velocity of the interacting atoms is changed by altering the pulse frequency. The resultant frequency shift contains information on the cavity phase-shift which can be calculated from Eq. (1). The second-order Doppler shift is trivial to calculate since the velocity V is known via the chosen pulse frequency from

$$V = L/T \qquad (2)$$

where T is the pulse period. Equation (2) is of course only exactly valid for infinitely narrow velocity windows. A correction may have to be applied if large windows are used [5], [8].

2) Beam Reversal: This method has been discussed in detail elsewhere [1], [11]. The beam is reversed which changes the sign of V_p in (1). Barring the knowledge of V_D and V_p for both beam directions this method alone would have to rely on the assumption that the reversed beam exactly retraces the previous beam trajectory, i.e., that full symmetry in the beam optics is present. Thus the ability to assure this condition would limit this method.
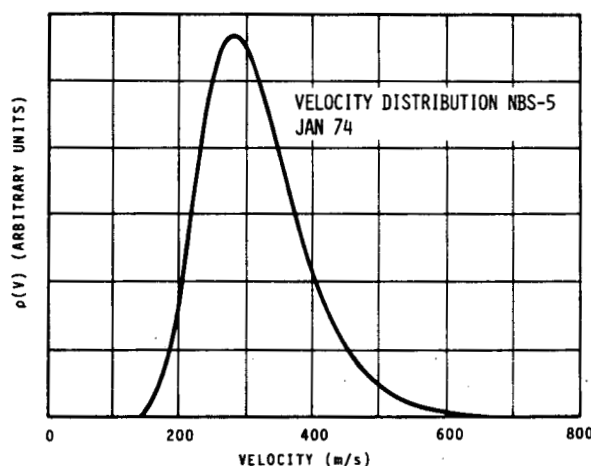

Fig. 15. Velocity distribution of NBS-5; on axis alignment. Measured by pulse method [2], [8], (velocity window: approximately 10 percent), and confirmed by analysis of Ramsey pattern [11].

We believe that the design of NBS-5 allows such retracing to a corresponding measurement accuracy in the velocity dependent effects of 1–2×10^{-13}. This is confirmed by the agreement among all three methods discussed (see Fig. 18). Beam reversal, combined with determinations of V_p could be developed to a very powerful evaluation method. We plan to pursue this avenue with NBS-5 and project, that the error in the determination of the velocity dependent biases can be reduced to below the 10^{-13} level. An extensive beam reversal analysis was performed in Sept./Oct. 1973 on NBS-5. The results from these data are in agreement, within measurement precision, with the other methods used to evaluate the cavity phase shift bias.

3) Power Shift: The following discusses in greater detail the microwave power-shift measurements which led to most of the values for the second-order Doppler and cavity phase-shift bias and the related uncertainties. As an example, data from the calibration of the NBS time scale in Jan. 1974 using NBS-5 are presented later. The procedures and techniques used for other power-shift evaluations of NBS-5 as well as NBS-4 are the same, differing only in the numerical values.

The velocity distribution is first acquired by using the pulse method [2], [8], [9], as well as an analysis of the Ramsey pattern [11]. The results from both methods agreed usually to within several percent. The velocity distribution of NBS-5 for the calibration data under discussion is shown in Fig. 15. (A velocity distribution for NBS-4 is shown in Fig. 16). From this distribution, the mean velocities V_p and V_D were calculated as a function of microwave excitation power. This is depicted in Fig. 17 where the excitation parameter bl (b is proportional to $(\text{Power})^{1/2}$) is used. Also plotted is the calculated dependence of the cesium signal intensity as a function of b. Fig. 17 allowed us to select two suitable power settings. We chose optimum power ($bl = 220$ ms^{-1}, l is the effective interaction length of one cavity section) and 4.6 dB above optimum power ($bl = 374$ ms^{-1}). The latter setting corresponds to the maxima of the V_p and V_D curves of Fig. 17,
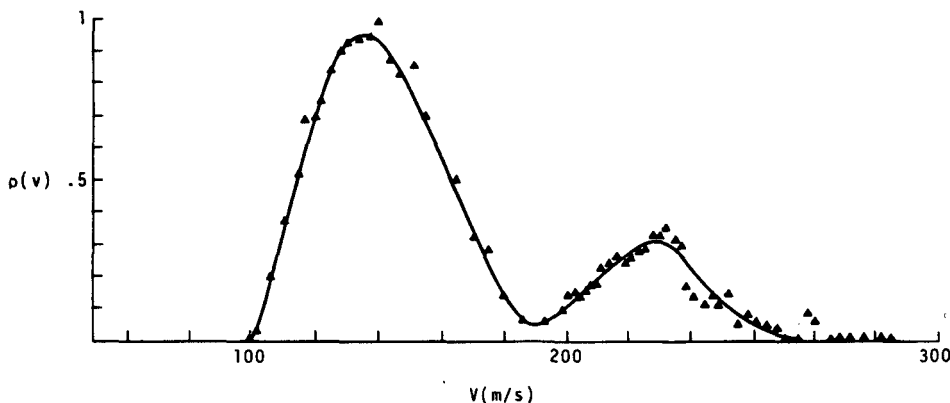
NBS-4

Fig. 16. Velocity distribution of NBS-4. Measured by pulse method [2], [8]. Pulse period was $\tau = 50$ μs. These data agree very well with those derived from analysis of NBS-4 Ramsey pattern [11].
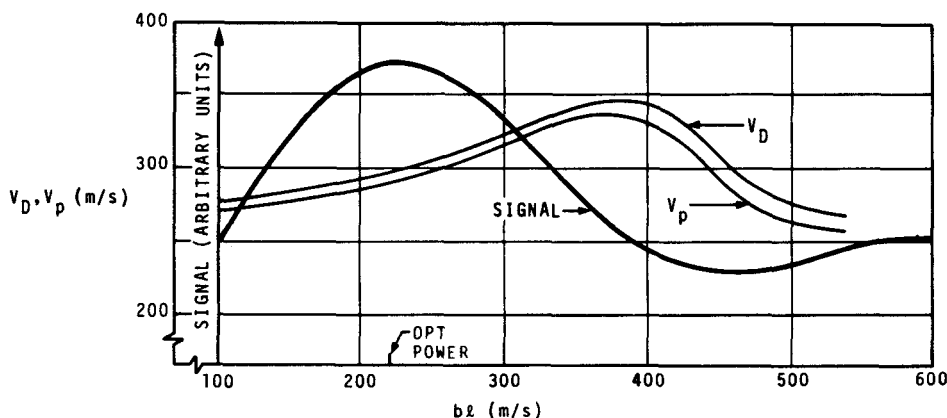
SIGNAL & MEAN VELOCITIES V_D, V_p NBS-5, JAN 74

Fig. 17. Mean velocities V_P and V_D as well as detector signal as function of microwave power parameter b calculated from velocity distribution of Fig. 15. Maximum signal occurs at optimum power, maximum mean velocities occur at 4.6 dB above optimum power. Diagram illustrates the selection of velocities with microwave power.

and thus offers a first-order independence from small uncertainties in this power setting. The resultant measured frequency shift (NBS-4 served as the reference) was (1.13 ± 0.28) mHz. The modulation amplitude of NBS-5 was set at nominally 18 Hz (36 Hz peak to peak). These data were processed in a computer program [11] with results as shown in Table II. Table II depicts the computer program printout. The first line shows the chosen bl values in cm/s (first two values), the modulation amplitude in Hz (third value), and the measured frequency shift in Hz (fourth value). The six values of the second line give successively (see Fig. 17) V_D at optimum power, V_D at +4.6 dB, V_D at the selected nominal power setting, V_p at optimum power, V_p at +4.6 dB, and V_p at the selected nominal setting. The third line depicts the total frequency bias computed from the above information for nominal (here optimum) power setting. The result is

$$\Delta\nu = -1.4 \text{ mHz}; \qquad \delta = -0.25 \text{ mrad}.$$

Since the velocities are known, one can extract the second-order Doppler bias. Using (1) we obtain $\Delta\nu_{\text{Doppler}} = -4.5$ mHz and $\Delta\nu_{\text{Phase}} = +3.1$ mHz. These two effects thus nearly cancel for the chosen beam direction of NBS-5.

The remainder of Table II depicts results leading to the assigned uncertainty for the aforementioned values. The data are presented in six blocks, each headed by the assumed modulation amplitude (varied by 1 Hz) and the assumed frequency-shift value (measured; and measured $\pm$ uncertainty).[4]

The first two columns give the low and high bl values and variations around them (± 0.1 dB). The third and fourth columns give the resultant value for the frequency bias and the cavity phase angle difference. We note that under the assumed variations the maximum and minimum

---

[4] The uncertainty is the 1σ measurement uncertainty in the power-shift experiment.

```
BHH.BLL.FR.JEL NOMINAL
   2.2000+004    3.7361+004    1.8000+001    1.1300-003
VUH.VUL.VUU.VPH.VPL.VPU.
  29624.93  34813.04  29624.93  29209.65  34002.04  29209.65

NOMINAL FREQ SHFT.PHS SHFT
  -0.00140215 -0.00025237

FR.OEL         1.8000+001 1.1300-003
BHH.BLL.FREQ SHFT.CAV PHSE
  22000.00  37361.36      -0.00140215 -0.00025237
  22000.00  37793.98      -0.00134795 -0.00025673
  22254.75  37361.36      -0.00149662 -0.00024583
FR.OEL         1.9000+001 1.1300-003
BHH.BLL.FREQ SHFT.CAV PHSE
  22000.00  37361.36      -0.00136960 -0.00025647
  22000.00  37793.98      -0.00130628 -0.00026167
  22254.75  37361.36      -0.00146276 -0.00025005
FR.OEL         1.8000+001 1.4100-003
BHH.BLL.FREQ SHFT.CAV PHSE
  22000.00  37361.36      -0.00310847 -0.00011498
  22000.00  37793.98      -0.00386210 -0.00011871
  22254.75  37361.36      -0.00323105 -0.00010651
FR.OEL         1.9000+001 1.4100-003
BHH.BLL.FREQ SHFT.CAV PHSE
  22000.00  37361.36      -0.00306987 -0.00012002
  22000.00  37793.98      -0.00300995 -0.00012483
  22254.75  37361.36      -0.00319073 -0.00011169
FR.OEL         1.8000+001 5.5000-004
BHH.BLL.FREQ SHFT.CAV PHSE
  22000.00  37361.36       0.00030416 -0.00038979
  22000.00  37793.98       0.00036628 -0.00039475
  22254.75  37361.36       0.00023781 -0.00038516
FR.OEL         1.9000+001 6.5000-004
BHH.BLL.FREQ SHFT.CAV PHSE
  22000.00  37361.36       0.00033067 -0.00039293
  22000.00  37793.98       0.00040018 -0.00039851
  22254.75  37361.36       0.00026521 -0.00038842
```

values for the frequency bias are -3.2 mHz and $+0.4$ mHz. We therefore quote an uncertainty of ±1.8 mHz or $\pm2 \times 10^{-13}$ for this particular measurement. The corresponding uncertainty in δ is ±0.15 mrad. We also note, as Table II clearly shows, that this uncertainty is mostly due to the measurement uncertainty of the frequency shift, i.e., the power-shift experiment itself. More extensive use of NBS-4 as the frequency reference will reduce further this uncertainty. The contributions of uncertainties in the power setting and the modulation amplitude are small and correspond to parts in 10^{14}.

MEASUREMENTS UTILIZING THE PRIMARY FREQUENCY STANDARDS

NBS-4 has been in operation since June 1973 and has served for calibrations of the NBS Atomic Time Scale since August 1973. NBS-5 has been operating since November 1972, and has been used for time scale calibrations since January 1973. NBS-5 has served in six independent, full calibrations using the three evaluation methods discussed earlier: beam reversal, pulsed operation, and power shift. NBS-4 has undergone two full individual evaluations based on the power shift method. The use of NBS-4 since then has involved only a limited accuracy evaluation. In these limited accuracy evaluations, only selected parameters are evaluated such as the magnetic field and the microwave spectrum. We rely thus on the cavity phase shift having remained constant since the last full evaluation. The reproducibility is estimated to be 1×10^{-13}. The bias-corrected frequencies of NBS-4 and NBS-5 agree, to within $(1 \pm 10) \times 10^{-13}$ with the value obtained for NBS-III in 1969, which value is preserved in the rate of the NBS Atomic Time Scale.

Fig. 18 summarizes the results of the calibrations using NBS-4 and NBS-5 since January 27, 1973, where zero on the ordinate corresponds to the rate of AT_0(NBS) at that time. AT_0(NBS) corresponds to UTC(NBS) with the principal difference that no intentional changes (such as those applied to UTC(NBS)) occur in AT_0(NBS). AT_0(NBS) is thus a reference scale as stable and uniform as can be provided by the NBS Atomic Clock Ensemble.

The error bars of the evaluations are included in the figures. The limited accuracy evaluations of NBS-4 were plotted with error bars equal to the uncertainty of the last full evaluation of NBS-4. Fig. 18 shows that in individual evaluations of NBS-5 values of 2×10^{-13} have been realized, while evaluations of NBS-4 reached 3×10^{-13}. If the assumption is made that the calibrations of AT_0(NBS) are statistically independent, one can obtain a better estimate of the accuracy of the reference such as AT_0(NBS), or the International Atomic Time (TAI) by statistically processing the data as a time series. One of the authors (Allan), has developed a filtering equation [13], which permits an optimum processing of such data. The result is plotted in Fig. 19. This figure combines all NBS-4 and NBS-5 calibrations since January 1973. The filtering was used on all previous data with appropriate weighting to obtain an improved number for any given calibration data.

Also plotted (crosses) are the original data corresponding to Fig. 18. The first cross is identical with the first "filtered" point. In the following data the filtering causes a smoothing of the time-series of calibrations. From Fig. 19 the final, achieved accuracy[5] after a series of 12 calibrations approaches an uncertainty of 1.3×10^{-13} which is much better than that of any single calibration. One also observes a drift in the atomic time scale AT_0(NBS) of about 2 parts in 10^{13} from January 1973 to the fall of 1973. Since September 1973 no systematic drift has been measured. This coincides with the implementation of a clock treatment as proposed by Barnes and Allan [14], which involves an occasional adjustment of the oscillator error voltage of each clock in the ensemble to be close to zero. This eliminates frequency drift in the locked system due to oscillator aging (nominally increasing error voltage) due to the finite gain of the servo loop. (See also the section on Electronics Systems and Frequency Stability.)

A plot similar to Fig. 19 is shown in Fig. 20 for the TAI, as measured at NBS via Loran-C. The error bars[5] for these plots include errors due to the propagation uncertainty in the Loran-C reception, and thus reflect uncertainty in addition to that of measurement with the primary standard alone. The apparent drift in TAI of 2 or 3 parts in 10^{13} from January 1973 to September 1973, lies well within the error bars of the measurement and may, therefore, be considered inconclusive. As shown in Fig. 20, the 1-sigma accuracy in the measurement of TAI (which includes the propagation uncertainty) is now 1.6×10^{13}. The best estimate at NBS of the rate of TAI in terms of the cesium

---

[5] The error bars of the first calibrations are larger than those in Fig. 18 due to the inclusion of NBS-III data from 1969 in the filtering process.
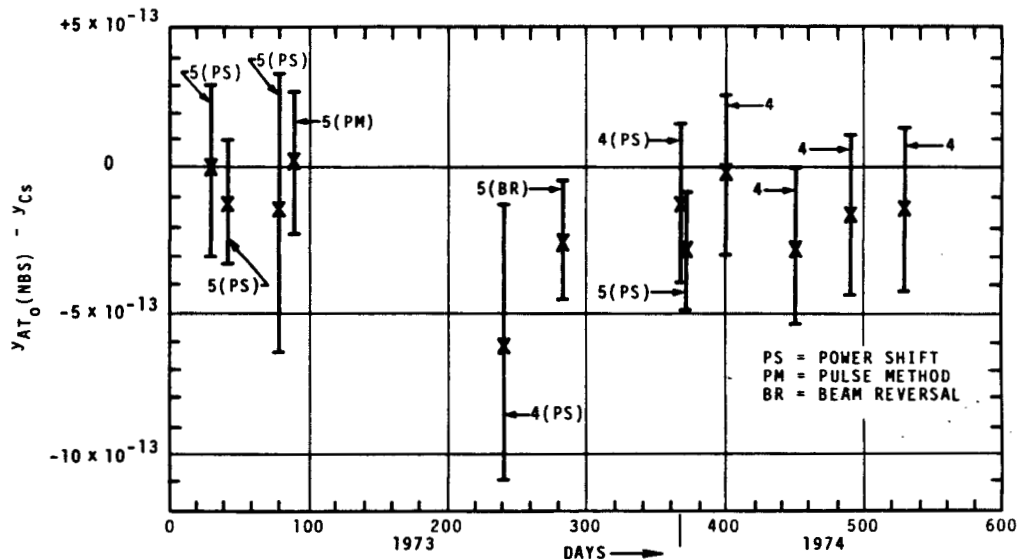
Fig. 18. Frequency calibrations of AT₀(NBS) using both NBS-4
and NBS-5 (Jan. 27, 1973–June 14, 1974). Data after day 380 are
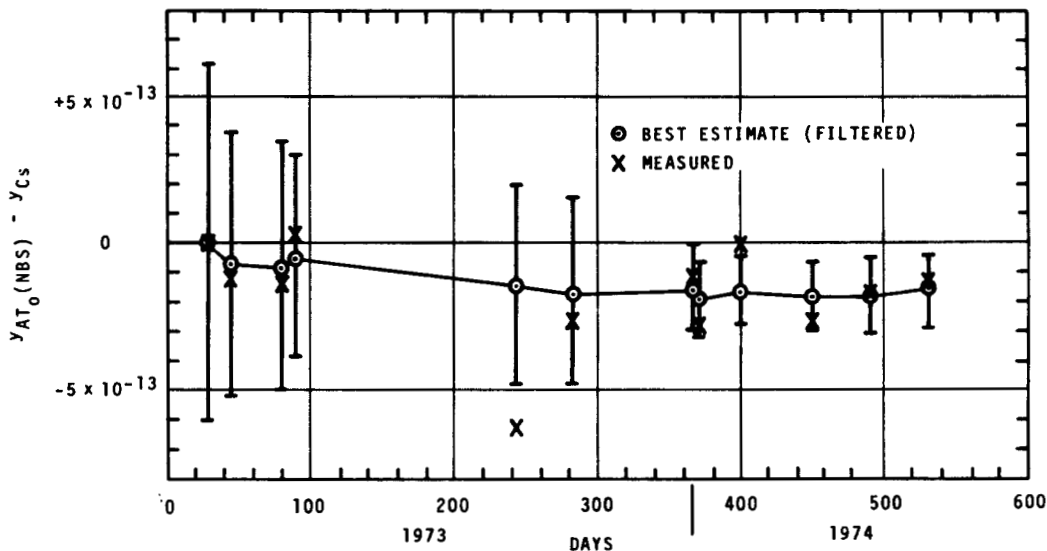for limited accuracy evaluations of NBS-4 (see text).

Fig. 19. Best estimate of frequency calibrations of AT₀(NBS)
(circles). Each data point contains the weighted input of all pre-
vious data points [13]. The raw measurement data of Fig. 18 are
indicated as crosses.

frequency is $+10.0 \times 10^{-13}$ since September 1973. We
have data available on the measurement of the PTB,
Germany, and the NRC, Canada, through the courtesy
of Becker and Mungall, respectively [12], [15]–[17]. For
the fall of 1973, it was thus possible to obtain a comparison
of the measurement of the rate of TAI by the three
laboratories operating primary, evaluated cesium stand-
ards. Table III shows the measurement results and the
individually quoted uncertainties. In the third column the
methods are listed which were used to evaluate the second-
order Doppler and cavity phase-shift biases. It is im-
portant to note that the PTB and NRC are located at
essentially sea level. The NBS in contrast is located at
approximately 1600 m above sea level; thus, the frequency

of TAI as seen at Boulder, Colo., appears too low due to
the effects of general relativity. We, therefore, applied to
the frequency of our cesium standards a gravitational
correction of -1.8×10^{-13}. This correction is included in
Table III and Fig. 20. Without this general relativity
correction, the frequency of TAI as measured in Boulder
would have been approximately 8×10^{-13}.

CONCLUSIONS

The initial comprehensive evaluation phase is now
completed for NBS-4 and NBS-5, and improvements and
better experiments are already being carried out. Results
have been encouraging, and knowledge of our standards
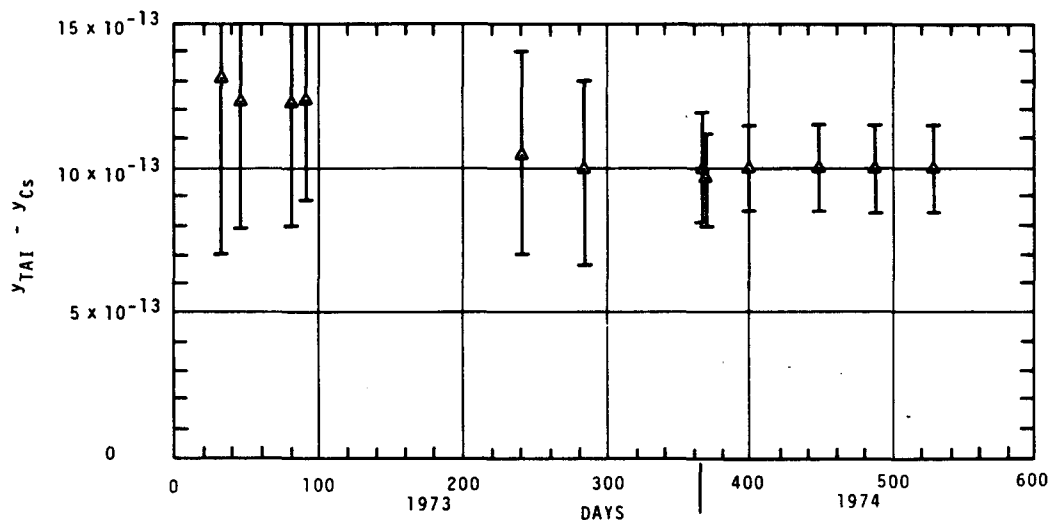and of those from other laboratories is increasing rapidly.

Fig. 20. Best estimate of frequency of TAI from the calibrations of Fig. 18. Each data point contains weighted input of all previous data points [13]. Uncertainties include Loran-C measurement uncertainty (1–2 × 10^{-13}).

INTERNATIONAL AGREEMENT...Cs STANDARDS
REF: FALL 1973

	TAI - Cs	1 SIGMA UNCERTAINTY	TECHNIQUE
PTB	11 x 10^{-13}	1.5 x 10^{-13}	BEAM OPTICS CHANGE BEAM REVERSAL
NRC	10 x 10^{-13}	1-2 x 10^{-13}	BEAM REVERSAL
NBS	10 x 10^{-13}	1.6 x 10^{-13}	BEAM REVERSAL MW POWER SHIFT PULSED MW OPERATION

It is not unreasonable to expect that documented accuracies of cesium devices may soon be better than 1×10^{-13}.

ACKNOWLEDGMENT

The authors wish to express sincere appreciation for the help of the late J. H. Holloway for many helpful discussions regarding beam optics design and other problems associated with cesium beam tubes. He was directly responsible for many contributions and developments in the NBS-4 beam tube, and his continued interest and support over several years have contributed very significantly to the success of this present work.

L. S. Cutler has contributed significantly to the NBS-4 and NBS-5 work in the areas of beam optics, electronics (especially on the double integrator and servo system), and C-field, and the authors appreciate his considerable help.

We wish to thank L. F. Mueller for the major responsibility in the redesign and construction of several components of the NBS-4 beam tube, and for its re-assembly and alignment. We also wish to thank him for his considerable help during the final assembly and testing phases for NBS-5.

R. F. Lacey and G. A. Seavey have also contributed significantly to the NBS-4 work, and their continuing interest over several years' time is appreciated.

H. E. Bell contributed significantly in wiring and assembly for both NBS-4 and NBS-5. His continuing involvement in both areas is greatly appreciated.

The authors wish to thank J. A. Barnes for his continuing interest in and contributions to the analyses and measurements associated with the electronics systems for the primary frequency standards.

The work of D. Halford in the areas of noise characterization, measurement, and reduction is greatly appreciated.

We also appreciate the efforts of W. D. McCaa, Jr., during the latter phase of the work and the efforts of H. F. Salazar on the diagnostic electronic systems. The work of C. S. Snider who helped on mechanical design and testing of the reversible beam system is also appreciated.

A special word of commendation should be given to W. T. Roberts who constructed almost all of the NBS-5 beam tube, and many of the components for NBS-4. His careful work, continued enthusiasm, and contributions to designs over several years' time have had a significant impact on the success of this work.

REFERENCES

[1] D. J. Glaze, "Improvements in atomic cesium beam frequency standards at the National Bureau of Standards," IEEE Trans. Instrum. Meas., vol. IM-19, pp. 156–160, Aug. 1970.
[2] H. Hellwig, S. Jarvis, Jr., D. Halford, and H. E. Bell, "Evaluation and operation of atomic beam tube frequency standards using time domain velocity selection modulation," Metrologia, vol. 9, no. 3, pp. 107–112 1973.
[3] R. F. Lacey, L. S. Cutler, and W. F. Turner, U. S. Patent 3 670 171.
[4] R. F. Lacey, "Phase shift in microwave Ramsey structures," in Proc. 22nd Annu. Symp. Freq. Contr., pp. 545–558, 1968.
[5] H. Hellwig, "Atomic frequency standards, a survey," in Proc. 28th Annu. Symp. Freq. Contr.
[6] L. S. Cutler, Hewlett–Packard Co., Palo, Alto CA, private commun., 1971.
[7] R. F. Lacey, A. L. Helgesson, and J. H. Holloway, "Short-term stability of passive atomic frequency standards," Proc. IEEE, vol. 54, pp. 170–176, Feb. 1966.
[8] D. A. Howe, H. E. Bell, Helmut Hellwig, and Andrea DeMarchi, "Preliminary research and development of the cesium tube

accuracy evaluation system," in *Proc. 28th Annu. Symp. Freq. Contr.*

[9] D. J. Glaze, A. E. Wainwright, and D. W. Allan, "Recent progress on the NBS primary frequency standard," in *Proc. 27th Annu. Symp. Freq. Contr.*, pp. 347–356, 1973.

[10] J. H. Holloway and R. F. Lacey, "Factors which limit the accuracy of cesium atomic beam frequency standards," in *Proc. Int. Conf. Chronometry*, pp. 319–331. 1964.

[11] S. Jarvis, Jr., "Determination of velocity distributions in molecular beam frequency standards from measured resonance curves," *Metrologia*, vol. 10, 1974.

[12] A. G. Mungall, R. Bailey, H. Daams, D. Morris, and C. C.

Costain, "The new NRC 2.1 metre primary cesium beam frequency standard, CS V," *Metrologia*, vol. 9, no. 3, pp. 113–117, 1973.

[13] D. W. Allan, NBS, Boulder, Co., private commun., 1974.

[14] J. A. Barnes, D. W. Allan, NBS, Boulder, Co., private commun., 1974.

[15] G. Becker, "Frequenzvergleiche mit dem primaren Zeit-und Frequenznormal CS1 der Physikalisch-Technischen Bundesanstalt Zwischen 1969 und 1973," *PTB-Mitteilungen*, vol. 83, no. 5, pp. 319–326, 1973.

[16] G. Becker, PTB, Braunschweig, Germany, private commun.

[17] A. Mungall, NRC, Ottawa, Canada, private commun.